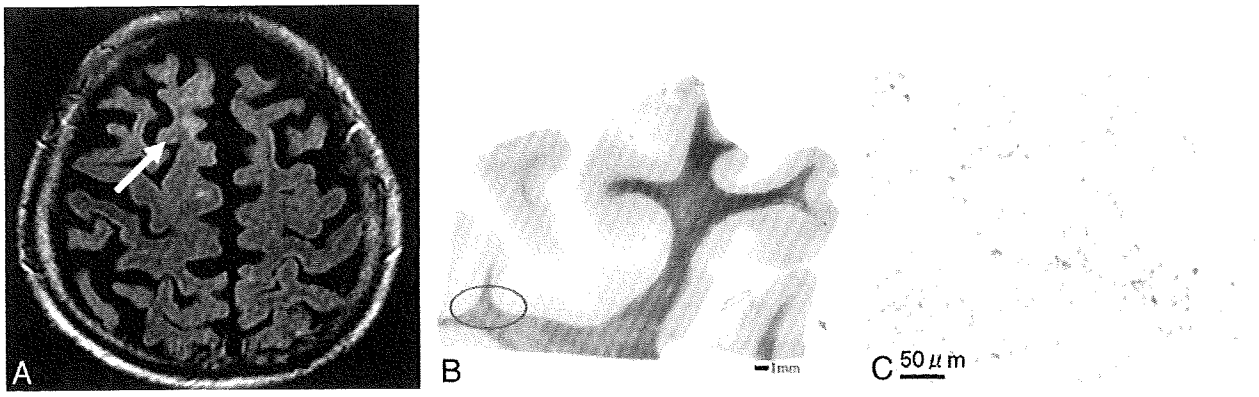

Fig 7. Corticobasal degeneration (CBD), case 1. An 84-year-old woman. *A*, Axial T2-weighted image shows a high signal intensity in the right frontal subcortical white matter (*white arrow*). *B*, In a microscopic specimen of the right frontal lobe corresponding to the site of white matter lesions, myelin sheath staining is decreased (*red oval*). The scale is 1 mm. *C*, In this area, there is positive staining for antiphosphorylated tau antibody on AT8 staining, which is compatible with the primary changes in CBD. The scale is 50 μm.

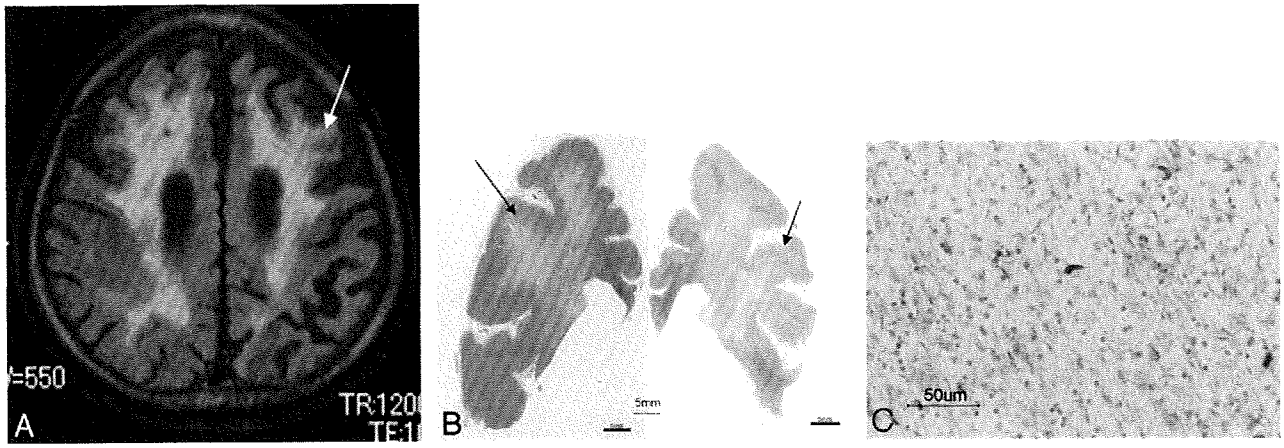

Fig 8. Corticobasal degeneration (CBD), case 3. A 70-year-old man. *A*, An axial fluid-attenuated inversion recovery image shows a high signal intensity bilaterally over a wide area in the frontal lobes (*arrow*). *B*, Corresponding to sites of white matter lesions, myelin sheath staining is decreased (*arrow*). The scale is 5 mm. *C*, These sites are stained positively for antiphosphorylated tau antibody. The scale is 50 μm. The changes are primary characteristics of CBD.

the early stage, but patients may be misdiagnosed due to a lack of cortical symptoms.[10-14] The above patient (case 2) may be an example of such a clinical presentation. Clinical evaluation showed little evidence of asymmetric cortical dysfunction, and neuropathology revealed only minimal cortical asymmetry. In this case, MR imaging showed a slight high signal intensity in the frontal SCWM; the midbrain tegmentum was severely atrophied, with an area of 71 mm^2; and T1-weighted imaging showed symmetric high-intensity signals in the subthalamic nucleus. Although a clear description is difficult on the basis of only 1 case, it was demonstrated by the pathologic findings that when identification of the cortical sign is difficult and unilateral atrophy is unclear on imaging, imaging findings, such as atrophy of the midbrain tegmentum, an abnormal signal intensity in the SCWM on FLAIR, or signal intensity changes in the subthalamic nuclei on T1-weighted imaging, may serve as supportive findings suggesting CBD.

CBD is important to differentiate from PSP. Oba et al[2] described a convenient and objective approach to diagnosing PSP based on midsagittal measurement of the midbrain tegmentum area. However, Koyama et al[1] also reported midbrain tegmentum atrophy in CBD. In our 4 cases of neuropathologically confirmed disease, severe midbrain tegmentum atrophy was also observed. Although there was a limited number of cases, because there was no individual overlap of the midbrain tegmental area between the healthy controls and patients with pathologically confirmed CBD and PSP, investigation of midbrain tegmental atrophy may have led to the diagnosis of CBD and PSP. Although no statistical analysis was performed because of the limited number of cases, it may be difficult to differentiate CBD from PSP on the basis of the presence of midbrain tegmental atrophy alone. A so-called "penguin sign" may be a distinguishing feature of PSP, but with severe midbrain tegmentum atrophy, both PSP and CBD must be considered. On neuropathology, there was marked depigmentation of the substantia nigra and locus ceruleus. Other findings included melanophagia and gliosis, and Gallyas-Braak silver staining revealed argyrophilic threads and granular or fibrous inclusion bodies. These findings were consistent with CBD as a cause of the atrophy. The degeneration of motor nerve nuclei, including the oculomotor and abducens nuclei, in the brain stem tegmentum was also noted, but no corresponding imaging findings were seen in the present study.

The localization of SCWM abnormalities, though different from those in previous reports,[1,15] was prominent in the present study. In CBD, Tokumaru et al,[15] Doi et al,[16] and Koyama et al[1] described predominantly unilateral SCWM abnormalities on T2-weighted imaging and FLAIR. In their re-

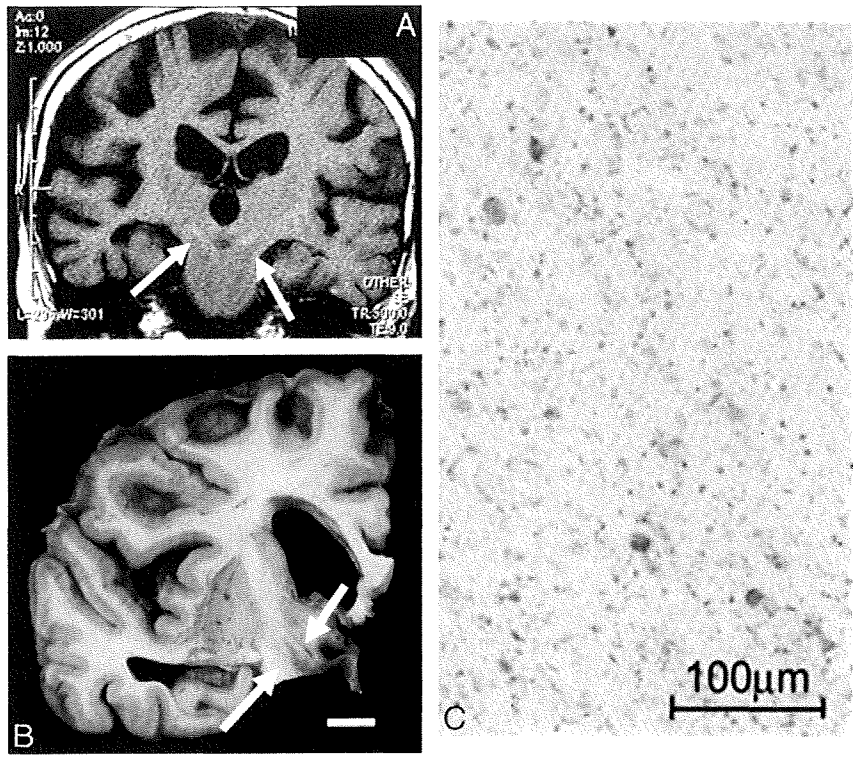

Fig 9. Corticobasal degeneration (CBD), case 1. An 84-year-old woman. *A*, Coronal T1-weighted image shows symmetric high signal intensity bilaterally in the subthalamic nuclei (*arrows*). *B*, A macroscopic specimen shows a brownish change in the subthalamic nuclei (*arrows*). *C*, On microscopic examination (AT8 stain), antiphosphorylated tau antibody–positive neurons and gliosis are observed. These changes are characteristic of CBD. The scale is 100 μm.

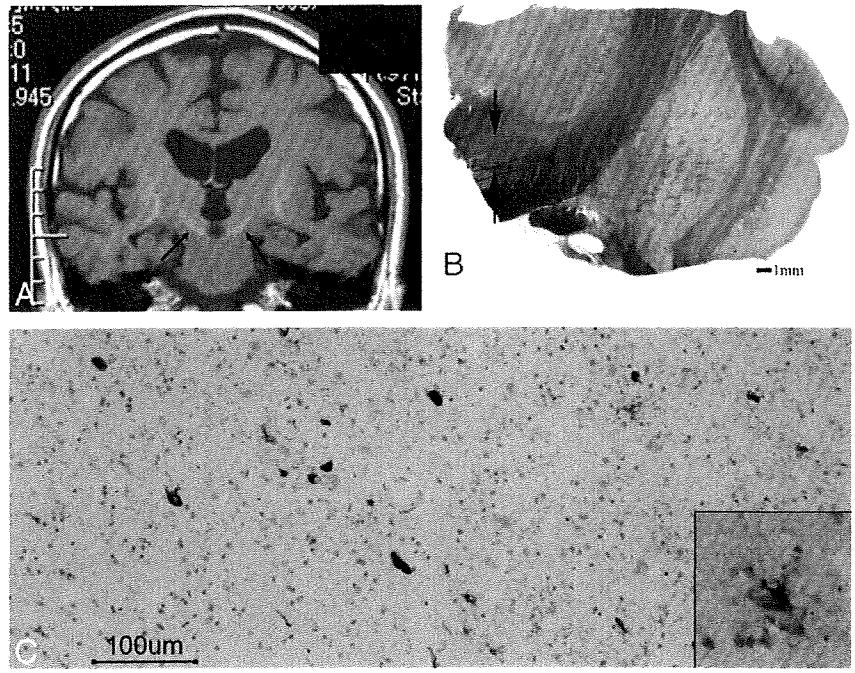

Fig 10. Progressive supranuclear palsy (PSP). An 84-year-old man. *A*, Coronal T1-weighted image shows a symmetric high signal intensity bilaterally in the subthalamic nuclei (*arrow*). *B*, A microscopic specimen of myelin-sheath staining shows the atrophic change of the subthalamic nuclei (*arrows*). The scale is 1 mm. *C*, On microscopic examination in the subthalamic nuclei, AT8 staining is clearly positive in the neurons (brown area). An enlarged image shows a tuft. These changes are characteristic of PSP. The scale is 100 μm.

ports, localization in the precentral gyrus of the SCWM and signal-intensity abnormalities contralateral to the clinically affected side were noted.[1,15] However, in the present study, the localization of white matter signal-intensity abnormalities differed among the 3 cases. In particular, in case 3, T2-weighted imaging and FLAIR showed widespread signal-intensity changes in the frontal lobe white matter bilaterally. This appearance differed from that reported by Doi et al[16] and Koyama et al.[1] In 2 patients, signal-intensity abnormalities were present in the superior frontal gyrus white matter. Only 1

patient showed signal-intensity abnormalities in the precentral gyrus SCWM. It is important to recognize the possibility of CBD showing different localizations of atrophy and white matter signal-intensity abnormalities rather than findings in the more typical cases as reported by Koyama et al.[1] In cases without predominantly unilateral cortical signs on clinical evaluation, the localization of atrophy and SCWM signal-intensity abnormalities may differ from typical cases. In these cases, MR imaging findings of high signal intensity in the subthalamic nucleus on T1-weighted images and severe atrophy of the midbrain tegmentum on midsagittal sections can provide useful information.

Rebeiz et al[17] first reported CBD with distinct features and a clinically asymmetric onset characterized by apraxia, dystonia, postural instability, and an akinetic-rigid syndrome that does not respond to levodopa, but since then, cases presenting with dementia, in which Alzheimer or Pick disease must be ruled out, and cases with other clinical features, in which PSP must be ruled out, have been reported.[18-21] A variety of underlying neuropathologic features have also been reported. Recent reports clarified the presence of many phenotypes of CBD neuropathologically and clinically.[10-14] Although there were only 4 cases, it was difficult to diagnose CBD clinically in cases definitely diagnosed neuropathologically, and 1 case showed imaging findings different from those previously reported. The lesions in the white matter widely expanded bilaterally in case 3, indicating that the clinical features alone did not confirm CBD. This case probably represents a new clinical phenotype of CBD.

Neuropathologic examination of SCWM lesions that correlated with the MR imaging findings showed the typical tauopathy of CBD. The degenerative changes were characteristic of CBD. In 1996, we suggested, on the basis of the neuropathologic findings in CBD, that white matter lesions of the frontal lobe were secondary degenerative changes.[15] Doi et al[16] and Koyama et al[1] also believe that these white matter lesions in CBD reflect the progression of neuronal degeneration, especially demyelination secondary to axonal loss or change. However, in the present study, at sites where MR imaging showed white matter lesions, though neuropathologic examination revealed some secondary degeneration, tauopathy in the white matter, particularly the SCWM, was clearly evident. This shows a positive radio-pathologic correlation of these changes in CBD. In 2002, Dickson et al[8] proposed neuropathologic criteria, with a primary emphasis on tau-positive neuronal and glial lesions, for the diagnosis of CBD. Advances in neuropathologic staining methods to evaluate tau have expanded our knowledge of these primary changes in CBD. Dickson et al also confirmed tauopathy of the white matter in CBD. After the report of Dickson et al, the neuropathologic evaluation criteria for lesions in the white matter apparently changed, and the finding that lesions in the white matter were primary degeneration in CBD, not secondary, may be important new information for the evaluation of an association with clinical and pathologic findings. In the present cases, degeneration was severe, affecting U-fibers, which should be investigated to collate with MR images.

T1-weighted images, obtained in 3 patients with CBD, showed symmetric high-intensity signals in the subthalamic nucleus. This finding was also present in a high proportion of patients with PSP, making an MR imaging–based differential diagnosis difficult. Neuropathology of sites corresponding to these signal-intensity changes showed tauopathy-related degeneration. Gliosis was also present, but on T2-weighted imaging and FLAIR, signal-intensity changes were difficult to detect. Only axial sections were obtained on T2-weighted imaging. These may have been insufficient to delineate the subthalamic nucleus adequately. In PSP, there was a high rate of similar findings, so these were not useful in the differential diagnosis. In all patients with PSP, the neuropathology showed more severe degeneration than in those with CBD. In addition to midbrain tegmentum atrophy, the localization of degeneration was similar in CBD to that seen in PSP. These signal-intensity changes were only visually evaluated by the neuroradiologists in the limited number of cases, but no signal-intensity change was noted in the pathologically healthy group, suggesting that primary degenerative findings of the individual diseases in the subthalamic nuclei and abnormal signals in this region are significant to some extent. However, differentiating CBD and PSP based on these findings alone is not possible. Therefore, a combination of imaging findings, including the presence of white matter signal-intensity changes and asymmetric atrophy, is important in correctly diagnosing CBD.

Conclusions

The correlation between radiologic and pathologic findings was investigated in patients with CBD, and MR imaging findings that could be used to differentiate CBD from PSP clinically were identified.

In CBD, midbrain tegmentum atrophy was severe, and degeneration in this area was correlated with the severity. However, this finding did not help in the differential diagnosis distinguishing CBD from PSP. T1-weighted imaging showed symmetric high-intensity signals in the subthalamic nucleus, but a large proportion of patients with PSP had a similar finding. On neuropathologic examination, each disorder showed characteristic degeneration. The degree of degeneration was more severe in PSP, but no imaging-based differences were observed. In CBD, there was a high rate of atrophy contralateral to the clinically affected side, with extension to the central sulcus. This suggests that the localization of atrophy differs depending on the underlying etiology. In PSP, unilateral atrophy was not a predominant finding.

MR imaging, FLAIR, and T2-weighted imaging showed high signal intensities in the SCWM. Previous studies have correlated this finding with secondary degeneration. The present study is the first to correlate these SCWM signal-intensity changes with primary degeneration in CBD. In addition, the localization of white matter lesions was correlated with a variety of clinical phenotypes. This suggests that there are CBD types other than those that are localized only to the precentral gyrus SCWM.

References

1. Koyama M, Yagishita A, Nakata Y, et al. **Imaging of corticobasal degeneration syndrome.** *Neuroradiology* 2007;49:905–12
2. Oba H, Yagishita A, Terada H, et al. **New and reliable MRI diagnosis for progressive supranuclear palsy.** *Neurology* 2005;28:2050–55
3. Saito Y, Murayama S. **Neuropathology of mild cognitive impairment.** *Neuropathology* 2007;27:578–84
4. Mirra SS, Heyman A, McKeel D, et al. **The Consortium to Establish a Registry**

for Alzheimer's Disease (CERAD). Part II. Standardization of the neuropathologic assessment of Alzheimer's disease. *Neurology* 1991;41:479–86
5. Saito Y, Ruberu NN, Sawabe M, et al. **Lewy body-related alpha-synucleinopathy in aging.** *J Neuropathol Exp Neurol* 2004;63:742–49
6. McKeith IG, Galasko D, Kosaka K, et al. **Consensus guidelines for the clinical and pathologic diagnosis of dementia with Lewy bodies (DLB): report of the consortium on DLB international workshop.** *Neurology* 1996;47:1113–24
7. Braak H, Braak E. **Neuropathological stageing of Alzheimer-related changes.** *Acta Neuropathol* 1991;82:239–59
8. Dickson DW, Bergeron C, Chin SS, et al. **Office of Rare Diseases Neuropathologic Criteria for corticobasal degeneration.** *J Neuropathol Exp Neurol* 2002;61:935–46
9. Hauw JJ, Daniel SE, Dickson D, et al. **Preliminary NINDS neuropathologic criteria for Steele-Richardson-Olszewski syndrome (progressive supranuclear palsy).** *Neurology* 1994;44:2015–19
10. Mathuranath PS, Xuereb JH, Bak T, et al. **Corticobasal ganglionic degeneration and/or frontotemporal dementia? A report of two overlap cases and review of literature.** *J Neurol Neurosurg Psychiatry* 2000;68:304–12
11. Grimes DA, Lang AE, Bergeron CB. **Dementia as the most common presentation of cortical-basal ganglionic degeneration.** *Neurology* 1999;53:1969–74
12. Schneider JA, Watts RL, Gearing M, et al. **Corticobasal degeneration: neuropathologic and clinical heterogeneity.** *Neurology* 1997;48:959:969
13. Rinne JO, Lee MS, Thompson PD, et al. **Corticobasal degeneration: a clinical study of 36 cases.** *Brain* 1994;117:1183–96
14. Bergeron C, Pollanen MS, Weyer L, et al. **Unusual clinical presentations of cortical-basal ganglionic degeneration.** *Ann Neurol* 1996;40:893–900
15. Tokumaru AM, O'uchi T, Kuru Y, et al. **Corticobasal degeneration: MR with histopathologic comparison.** *AJNR Am J Neuroradiol* 1996;17:1849–52
16. Doi T, Iwasa K, Makifuchi T, et al. **White matter hyperintensities on MRI in a patient with corticobasal degeneration.** *Acta Neurol Scand* 1999;99:199–201
17. Rebeiz JJ, Kolodny EH, Richardson EP Jr. **Corticodentatonigral degeneration with neuronal achromasia: a progressive disorder of late adult life.** *Trans Am Neurol Assoc* 1967;92:23–26
18. Brown J, Lantos PL, Roques P, et al. **Familial dementia with swollen achromatic neuron and corticobasal inclusion bodies: a clinical and pathological study.** *J Neurol Sci* 1996;135:21–30
19. Doran M, du Plessis DG, Enevoldson TP, et al. **Pathological heterogeneity of clinically diagnosed corticobasal degeneration.** *J Neurol Sci* 2003;216:127–34
20. Feany MB, Mattiace LA, Dickson DW. **Neuropathologic overlap of progressive supranuclear palsy, Pick's disease, and corticobasal degeneration.** *J Neuropathol Exp Neurol* 1996;55:53–67
21. Jendroska K, Rossor MN, Mathias CJ, et al. **Morphological overlap between corticobasal degeneration and Pick's disease: a clinicopathological report.** *Mov Disord* 1995;10:111–14

Eur J Nucl Med Mol Imaging (2010) 37:3–11
DOI 10.1007/s00259-009-1202-1

ORIGINAL ARTICLE

Validation of cardiac ^{123}I-MIBG scintigraphy in patients with Parkinson's disease who were diagnosed with dopamine PET

Kenji Ishibashi · Yuko Saito · Shigeo Murayama · Kazutomi Kanemaru · Keiichi Oda · Kiichi Ishiwata · Hidehiro Mizusawa · Kenji Ishii

Received: 11 March 2009 / Accepted: 9 June 2009 / Published online: 22 July 2009

Abstract
Purpose The aim of this study was to evaluate the diagnostic potential of cardiac ^{123}I-labelled metaiodobenzylguanidine (^{123}I-MIBG) scintigraphy in idiopathic Parkinson's disease (PD). The diagnosis was confirmed by positron emission tomography (PET) imaging with ^{11}C-labelled 2β-carbomethoxy-3β-(4-fluorophenyl)-tropane (^{11}C-CFT) and ^{11}C-raclopride (together designated as dopamine PET).
Methods Cardiac ^{123}I-MIBG scintigraphy and dopamine PET were performed for 39 parkinsonian patients. To estimate the cardiac ^{123}I-MIBG uptake, heart to mediastinum (H/M) ratios in early and delayed images were calculated. On the basis of established clinical criteria and our dopamine PET findings, 24 patients were classified into the PD group and 15 into the non-PD (NPD) group.
Results Both early and delayed images showed that the H/M ratios were significantly lower in the PD group than in the NPD group. When the optimal cut-off levels of the H/M ratio were set at 1.95 and 1.60 in the early and delayed images, respectively, by receiver-operating characteristic analysis, the sensitivity of cardiac ^{123}I-MIBG scintigraphy for the diagnosis of PD was 79.2 and 70.8% and the specificity was 93.3 and 93.3% in the early and delayed images, respectively. In the Hoehn and Yahr 1 and 2 PD patients, the sensitivity decreased by 69.2 and 53.8% in the early and delayed images, respectively.
Conclusion In early PD cases, cardiac ^{123}I-MIBG scintigraphy is of limited value in the diagnosis, because of its relatively lower sensitivity. However, because of its high specificity for the overall cases, cardiac ^{123}I-MIBG scintigraphy may assist in the diagnosis of PD in a complementary role with the dopaminergic neuroimaging.

Keywords ^{123}I-MIBG · ^{11}C-CFT · ^{11}C-Raclopride · Scintigraphy · Positron emission tomography · Parkinson's disease

An Editorial Commentary on this paper is available at http://dx.doi.org/10.1007/s00259-009-1215-9.

K. Ishibashi · H. Mizusawa
Department of Neurology and Neurological Science,
Graduate School, Tokyo Medical and Dental University,
Tokyo, Japan

K. Ishibashi · K. Oda · K. Ishiwata · K. Ishii (✉)
Positron Medical Center,
Tokyo Metropolitan Institute of Gerontology,
1-1 Nakacho, Itabashi-ku,
Tokyo 173-0022, Japan
e-mail: ishii@pet.tmig.or.jp

Y. Saito
Department of Pathology, Tokyo Metropolitan Geriatric Hospital,
Tokyo, Japan

Y. Saito · S. Murayama
Department of Neuropathology,
Tokyo Metropolitan Institute of Gerontology,
Tokyo, Japan

K. Kanemaru
Department of Neurology, Tokyo Metropolitan Geriatric Hospital,
Tokyo, Japan

Introduction

Cardiac ^{123}I-labelled metaiodobenzylguanidine (^{123}I-MIBG) scintigraphy has been suggested to be useful for the diagnosis of idiopathic Parkinson's disease (PD), because many recent studies have revealed that cardiac ^{123}I-MIBG uptake decreases with disease progression and that almost all

patients in the advanced stage of PD show decreased cardiac ^{123}I-MIBG uptake [1–5]. However, it is unclear whether cardiac ^{123}I-MIBG uptake is a good surrogate marker for the diagnosis of PD, especially in early and mild PD cases, which are the most difficult to diagnose in daily clinical practice, because the data on the reduction of cardiac ^{123}I-MIBG uptake in the early stage of PD vary greatly among different studies [1–8]. Therefore, we aimed to investigate the sensitivity and specificity of cardiac ^{123}I-MIBG scintigraphy in diagnosing PD, focusing on early and mild cases of PD in the Hoehn and Yahr (HY) stages 1 and 2.

While planning this study, we focused on dividing the patients into PD and non-PD (NPD) groups in the most appropriate manner in order to acquire precise results. Previous studies have shown that the usual clinical diagnostic accuracy of PD ranges from 70 to 90%, and the accuracy rate greatly decreases in early cases [9–12]. In vivo neurofunctional imaging of the basal ganglia, which provides images of both pre- and postsynaptic nigrostriatal dopaminergic functions, has been recognized as a standard marker for the diagnosis of PD in every clinical stage [13–25]. Therefore, in order to improve the accuracy of the diagnosis of PD, especially in early PD cases, and to classify the patients into the PD and NPD groups in a more appropriate manner, we performed positron emission tomography (PET) imaging with ^{11}C-labelled 2β-carbomethoxy-3β-(4-fluorophenyl)-tropane (^{11}C-CFT) and ^{11}C-raclopride. PET imaging with ^{11}C-CFT and ^{11}C-raclopride can assess the levels of presynaptic dopamine transporter (DAT) and postsynaptic dopamine D_2-like receptor (D_2R), respectively, in the striatum. The two types of PET imaging techniques were together designated as dopamine PET. Further, we proposed the definitions of PD and NPD patterns in dopamine PET findings on the basis of the results which had been confirmed by previous studies.

We also investigated the association between cardiac sympathetic function assessed by cardiac ^{123}I-MIBG uptake, presynaptic nigrostriatal dopaminergic function assessed by striatal ^{11}C-CFT uptake and disease stage determined according to the HY scale.

Materials and methods

Subjects

The present study was a retrospective study. The subjects comprised 39 patients who visited the neurological outpatient clinic at Tokyo Metropolitan Geriatric Hospital from November 2001 to October 2007. They chiefly complained of one or more parkinsonian symptoms, including resting tremor, rigidity, bradykinesia and postural instability. The patients were divided into PD and NPD groups (Fig. 1). Cardiac ^{123}I-MIBG scintigraphy, dopamine PET and magnetic resonance imaging (MRI) were performed for all patients. None of the patients had any concomitant hereditary disorder that could cause parkinsonian symptoms. None of the patients had an individual history of any heart disease. Further, none of the patients were on any medication that could cause parkinsonian symptoms.

For dopamine PET, eight healthy subjects (five men and three women) aged 55–74 years [mean±standard deviation (SD) = 62.3±6.9 years)]were considered as controls. They were deemed healthy based on their medical history, physical and neurological examinations and MRI of the brain. Further, none of them were on medication.

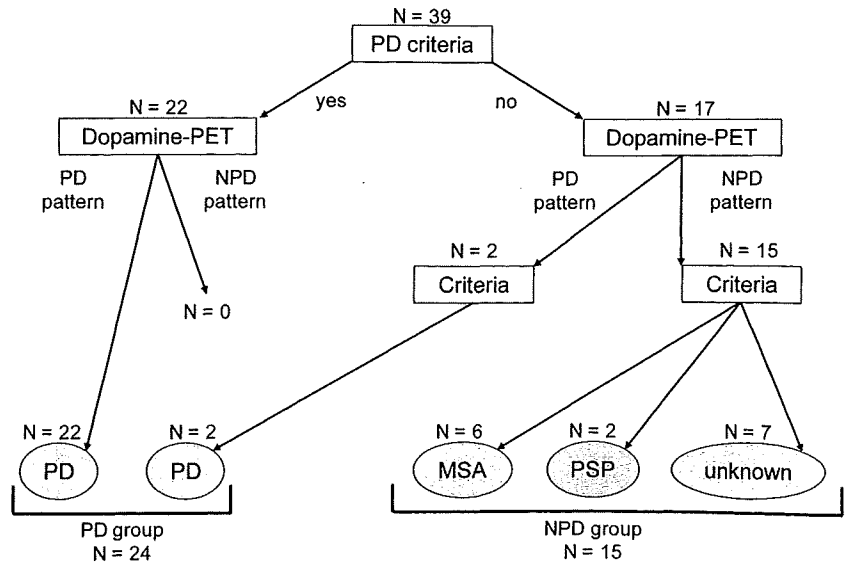

Fig. 1 Diagnostic flow chart and schematic representation of classification process. Patients were classified into PD and NPD groups on the basis of respective published clinical criteria and our dopamine PET findings

This study protocol was approved by the Ethics Committee of the Tokyo Metropolitan Institute of Gerontology. Written informed consent was obtained from all participants.

PET imaging

PET imaging was performed at the Positron Medical Center, Tokyo Metropolitan Institute of Gerontology by using a SET-2400 W scanner (Shimadzu, Kyoto, Japan) in the three-dimensional scanning mode [26], as described previously [27, 28]. The transmission data were acquired using a rotating $^{68}Ga/^{68}Ge$ rod source for attenuation correction. Images of 50 slices were obtained with a resolution of 2×2×3.125 mm voxels and a 128×128 matrix.

Dopamine PET imaging ^{11}C-CFT and ^{11}C-raclopride were prepared as described previously [29, 30]. The two types of PET imaging were performed for all of the subjects on the same day. The patients being treated with antiparkinsonian drugs underwent dopamine PET following at least 15 h deprivation of the medications. Each subject was administered an intravenous bolus injection of 341±62 (mean ± SD) MBq of ^{11}C-CFT, followed by that of 311±56 (mean ± SD) MBq of ^{11}C-raclopride after 2.5–3 h. To measure the uptake of the tracers, static scanning was performed for 75–90 and 40–55 min after the injection of ^{11}C-CFT and ^{11}C-raclopride, respectively. The specific activity of ^{11}C-CFT and ^{11}C-raclopride at the time of injection ranged from 5.9 to 134.2 GBq/μmol and from 10.2 to 201.7 GBq/μmol, respectively.

Analysis of dopamine PET images Image manipulations were performed using Dr. View version R2.0 (AJS, Tokyo, Japan) and SPM2 (Functional Imaging Laboratory, London, UK) implemented in MATLAB version 7.0.1 (The MathWorks, Natick, MA, USA).

The two PET images and one MRI image obtained for each subject were coregistered. The three coregistered images were resliced transaxially, parallel to the anteroposterior intercommissural (AC-PC) line. Circular regions of interest (ROIs) were selected with reference to the brain atlas and individually coregistered MRI images. In each of the three contiguous slices, one ROI with 8-mm diameter was selected on the caudate, two ROIs on the anterior putamen and two on the posterior putamen on both the left and right sides. In other words, the AC-PC plane and regions 3.1 and 6.2 mm above the AC-PC line were selected. A total of 50 ROIs with 10-mm diameter were selected throughout the cerebellar cortex in five contiguous slices.

To evaluate the uptake of ^{11}C-CFT and ^{11}C-raclopride, we calculated the uptake ratio index by the following formula [15, 31]: uptake ratio index = (activity in each region − activity in the cerebellum)/(activity in the cerebellum). We previously validated the method to estimate the binding potential of ^{11}C-raclopride and ^{11}C-CFT, adopting the uptake ratio index [27, 28]. For the further analyses, the uptake of each tracer in each subregion of the striatum (the caudate, anterior putamen and posterior putamen) was evaluated as the average value of the left and right sides. The uptake of each tracer in the whole striatum was evaluated as the average value of entire ROIs in the whole striatum.

Cardiac ^{123}I-MIBG scintigraphy

Scintigraphic studies were performed at Tokyo Metropolitan Geriatric Hospital by using a triple-headed gamma camera (PRISM-3000, Shimadzu, Kyoto, Japan). None of the patients were on any medication, i.e. they were not receiving any drugs such as antidepressants and monoamine oxidase inhibitors, which might influence cardiac ^{123}I-MIBG uptake. After a 30-min resting period, each patient was administered an intravenous bolus injection of 111 MBq of ^{123}I-MIBG (Fujifilm RI Pharma Co., Tokyo, Japan). Planar images of the chest in the anterior view were obtained twice for 5 min, starting at 20 min (early phase) and then at 180 min (delayed phase) after the injection of ^{123}I-MIBG. Relative organ uptake of ^{123}I-MIBG was determined by selecting the ROIs on the heart and mediastinum in the anterior planar image [32]. Average counts per pixel in the heart and mediastinum were used to calculate the heart to mediastinum (H/M) ratio.

MRI

MRI was performed at Tokyo Metropolitan Geriatric Hospital. By using a 1.5-T Signa EXCITE HD scanner (GE, Milwaukee, WI, USA), transaxial T1-weighted images [three-dimensional spoiled gradient-recalled (3D SPGR), repetition time (TR) = 9.2 ms, echo time (TE) = 2.0 ms, matrix size = 256 × 256 × 124, voxel size = 0.94 × 0.94 × 1.3mm] and transaxial T2-weighted images (first spin echo, TR= 3,000 ms, TE=100 ms, matrix size = 256 × 256 × 20, voxel size = 0.7 × 0.7 × 6.5mm) were obtained.

Clinical diagnosis

The diagnostic flow chart is shown in Fig. 1. First, the patients were divided into two groups (22 patients in one group and 17 patients in the other) on the basis of the clinical criteria of the UK Parkinson's Disease Brain Bank (UKPDBB) [10]. Each group was then further classified on the basis of dopamine PET findings. As shown in Fig. 2, the PD pattern in dopamine PET was defined as follows: (1)

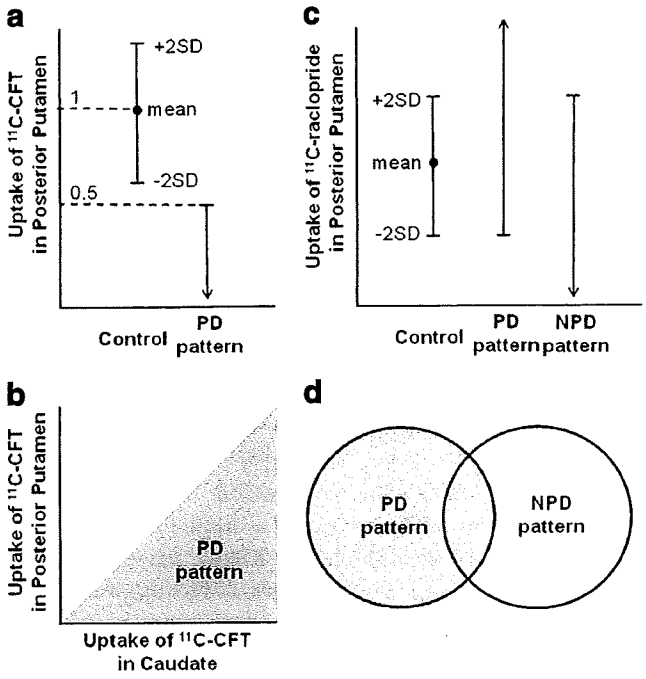

Fig. 2 PD and NPD patterns defined on the basis of dopamine PET findings. PD pattern: ^{11}C-CFT uptake in the posterior putamen of patients less than 50% of the mean uptake in the posterior putamen of normal controls (**a**) and less than that in the caudate of patients (**b**); ^{11}C-raclopride uptake in the posterior putamen of patients more than the mean – 2 SD of the uptake in the posterior putamen of normal controls (**c**). NPD pattern: ^{11}C-raclopride uptake in the posterior putamen of patients less than the mean + 2 SD of the uptake in the posterior putamen of normal controls (**c**). The patient was considered to be PD pattern when both PD and NPD were fulfilled (**d**). The uptake in each subregion of the striatum was evaluated as the average value of both sides

^{11}C-CFT uptake in the posterior putamen of the patients less than 50% of the mean uptake in the posterior putamen of normal controls (Fig. 2a) and less than that in the caudate of the patients (Fig. 2b) and (2) ^{11}C-raclopride uptake in the posterior putamen of the patients more than the mean – 2 SD of the uptake in the posterior putamen of normal controls (Fig. 2c). The NPD pattern was defined as follows: ^{11}C-raclopride uptake in the posterior putamen of the patients less than the mean + 2 SD of the uptake in the posterior putamen of normal controls (Fig. 2c). The patient was considered to be PD pattern when both PD and NPD were fulfilled (Fig. 2d).

Statistical analysis

Differences in the averages and variances were tested by Student's *t* test and one-way analysis of variance, respectively. Correlations between the two groups of patients were assessed by linear regression analysis with Pearson's correlation test; *p* values of <0.05 were considered statistically significant.

Results

Patients

Classification into PD and NPD groups All 22 patients who fulfilled the UKPDBB PD criteria at initial diagnosis [10] showed the PD pattern on dopamine PET (Fig. 1). They were classified into the PD group. The other 17 patients were further classified according to dopamine PET findings and respective published clinical criteria. Of the 17 patients, 2 showed the PD pattern on dopamine PET. In fact, the symptom manifested was only resting tremor at initial diagnosis; however, during the course of the study, they fulfilled the UKPDBB PD criteria [10] and were classified into the PD group.

Of the 17 patients, 15 showed the NPD pattern on dopamine PET and were classified into the NPD group (Fig. 1). These patients were then further divided into three subgroups. Six patients fulfilled the multiple system atrophy (MSA) criteria [33]. Two patients fulfilled the progressive supranuclear palsy (PSP) criteria [34]. For the remaining seven patients, no definitive diagnoses could be established despite follow-up for more than 1 year.

Finally, 24 patients (7 men and 17 women, age range: 60–85 years, mean age ± SD = 71.5±6.8 years) and 15 patients (8 men and 7 women, age range: 65–86 years, mean age ± SD: 76.0±5.5 years) were classified into the PD and NPD groups, respectively.

Demographic data Patient characteristics are summarized in Table 1. In the PD group, 11 patients were drug naive, 7 were being treated with L-dopa and 6 were being treated with L-dopa and dopamine agonists at the time of dopamine PET. The interval between cardiac ^{123}I-MIBG scintigraphy and dopamine PET was within 6 months for 16 patients, between 6 and 12 months for 1 patient and more than 1 year for 7 patients. However, the HY stage of each patient in the PD group remained the same between cardiac ^{123}I-MIBG scintigraphy and dopamine PET. In the NPD group, 11 patients were not administered any antiparkinsonian drug, and 4 were being treated with only L-dopa. The interval between the two examinations was within 6 months for 12 patients, between 6 and 12 months for 1 patient and more than 1 year for 2 patients.

Uptake of ^{123}I-MIBG

Both the early and delayed images showed significantly lower H/M ratios in the PD group than in the NPD group (Fig. 3). In both the early and delayed images, the H/M ratios tended to decrease with the progression of the HY stages; however, the decrease was not statistically significant.

Table 1 Clinical features of patients in Parkinson's disease and non-Parkinson's disease groups

Groups	Patients		Age (years)	Duration (years)	^{123}I-MIBG scintigraphy		^{11}C-CFT PET
	Number	M:F			Heart to mediastinum ratio		Uptake ratio index in the whole striatum
					Early	Delayed	
Parkinson's disease	24	7:17	71.5±6.8	3.5±3.2	1.66±0.45	1.46±0.41	0.98±0.34
Hoehn and Yahr 1	4	0:4	65.0±7.7	2.9±2.6	1.75±0.33	1.49±0.29	1.49±0.40
Hoehn and Yahr 2	9	2:7	73.9±5.6	2.4±1.0	1.81±0.54	1.60±0.45	1.00±0.20
Hoehn and Yahr 3	8	5:3	71.9±7.2	3.0±1.8	1.57±0.44	1.41±0.44	0.81±0.20
Hoehn and Yahr 4	3	0:3	72.3±5.0	9.0±6.1	1.36±0.05	1.12±0.08	0.69±0.07
Non-Parkinson's disease	15	8:7	76.0±5.5	2.8±1.9	2.35±0.46	2.18±0.51	1.65±0.68

Data are expressed as mean±SD

Table 2 shows the sensitivity and specificity of cardiac ^{123}I-MIBG scintigraphy in differentiating patients with PD from the other patients with chief complaints of parkinsonian symptoms. When the optimal cut-off levels of ^{123}I-MIBG were set at 1.95 and 1.60 by receiver-operating characteristic analysis, the sensitivity of cardiac ^{123}I-MIBG scintigraphy for the diagnosis of PD was 79.2 and 70.8% and the specificity was 93.3 and 93.3% in the early image and delayed images, respectively. In HY 1 and 2 PD patients the sensitivity was 69.2 and 53.9% and in HY 3 and 4 PD patients the sensitivity was 90.9 and 90.9% in the early image and delayed images, respectively

Uptake of ^{11}C-CFT

The uptake of ^{11}C-CFT in the whole striatum decreased with the progression of the HY stages (Fig. 4). Significant reduction in the ^{11}C-CFT uptake with the progression of the HY stages was also observed in each of the three subregions of the striatum. Correlation between cardiac ^{123}I-MIBG scintigraphy and ^{11}C-CFT PET was evaluated in the 16 patients who underwent the two examinations within 6 months. There was no significant correlation between the ^{11}C-CFT uptake in the whole striatum and the H/M ratios in both the early images (r=0.15, p=0.59) and delayed images (r=0.21, p=0.43) (Fig. 5). Further, no significant correlation was observed between the ^{11}C-CFT uptake in each of the three subregions of the striatum and the H/M ratio.

Discussion

In the present study, we investigated the sensitivity and specificity of cardiac ^{123}I-MIBG scintigraphy in diagnosing PD and differentiating the patients with PD from the others with chief complaints of parkinsonian symptoms. Further, we investigated the correlation between cardiac sympathetic function assessed by cardiac ^{123}I-MIBG uptake, nigrostriatal

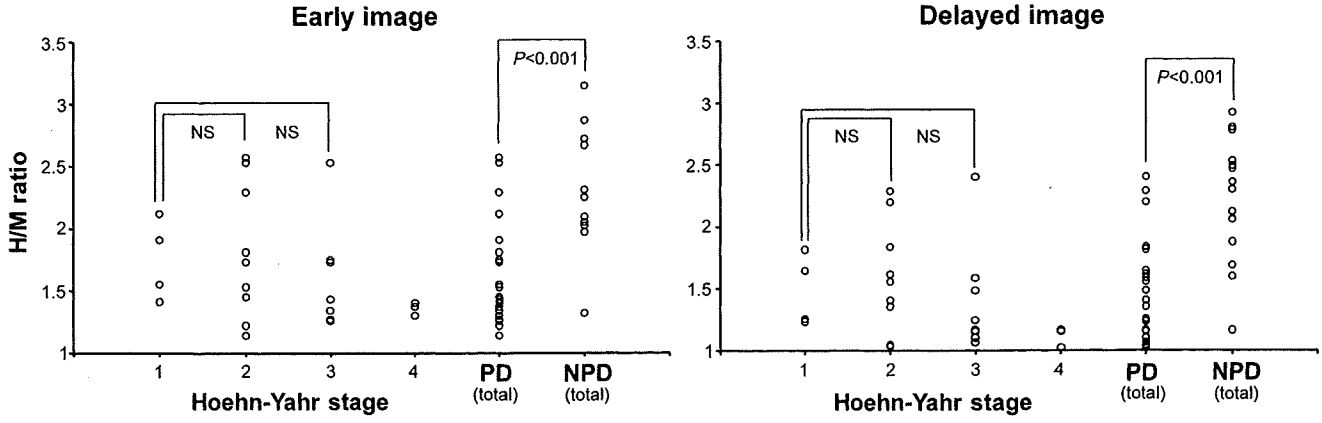

Fig. 3 H/M ratios in the PD and NPD groups in early and delayed images. Each graph represents the relation between the H/M ratio and Hoehn and Yahr stage of PD and a comparison of the H/M ratios of the total number of PD and NPD patients. Both images showed that the H/M ratios were significantly lower in the PD group than in the NPD group; however, the H/M ratios of patients in HY 1 of PD were not significantly higher than those of the patients in HY 2 and 3 of PD. *NS* not significant

Table 2 Sensitivity and specificity of cardiac ^{123}I-MIBG scintigraphy in differentiating Parkinson's disease from other parkinsonian syndromes

Total PD patients (n=24)												
	Early image						Delayed image					
Cut-off	1.80	1.85	1.90	1.95	2.00	2.05	1.60	1.65	1.70	1.75	1.80	1.85
Sensitivity	70.8%	75.0%	75.0%	79.2%	79.2%	79.2%	70.8%	75.0%	79.2%	79.2%	79.2%	87.5%
Specificity	93.3%	93.3%	93.3%	93.3%	86.7%	80.0%	93.3%	80.0%	73.3%	73.3%	73.3%	73.3%
Hoehn and Yahr 1 and 2 (n=15)												
	Early image						Delayed image					
Cut-off	1.80	1.85	1.90	1.95	2.00	2.05	1.60	1.65	1.70	1.75	1.80	1.85
Sensitivity	53.8%	61.5%	61.5%	69.2%	69.2%	69.2%	53.8%	61.5%	69.2%	69.2%	69.2%	84.6%

Cut-off levels, for which both the sensitivity and specificity were more than 70%, are shown. The optimal cut-off levels determined by receiver-operating characteristic analysis were at 1.95 and 1.60 in the early and delayed images, respectively

dopaminergic function assessed by ^{11}C-CFT uptake and disease stage determined according to the HY scale.

It has been reported that cardiac ^{123}I-MIBG uptake in patients with PD is significantly lower than that in patients with other parkinsonian syndromes [1–7]; this result corresponds to our results. Several reports suggest that the severity of motor impairment and disease duration are correlated with reduced ^{123}I-MIBG uptake in patients with PD [1, 2, 5, 6]; however, some other findings deny such correlations, similar to ours [3, 4, 7, 8]. This discrepancy is presumably explained by the fact that the degree of cardiac ^{123}I-MIBG uptake in patients in HY 1 and 2 of PD varies greatly among different studies. Difficult definitive diagnosis of PD in early and mild cases may also be because of the great variation. On the other hand, almost all patients in the advanced stage of PD have shown very low ^{123}I-MIBG uptake in both the previous and the present studies. Li et al. reported that cardiac sympathetic denervation progresses over time and that the rate of decrease in the number of sympathetic terminals appears to be at least as high as that of nigrostriatal dopaminergic terminals [35]. Therefore, we considered that although the onset of cardiac sympathetic denervation varied among the patients with PD, severe cardiac sympathetic denervation occurred in all of the patients by the terminal stage of PD. In regard to the association with a sympathetic symptom, it was reported that reduced ^{123}I-MIBG uptake does not always mean the existence of a sympathetic symptom [1, 3, 4, 7]. Also in this study, of the three patients in stage 4 of the HY scale who showed very low ^{123}I-MIBG uptake (Fig. 3), two had orthostatic hypotension; however, the remaining one patient had no cardiovascular sympathetic symptom and showed no abnormality in the head-up tilt test. In contrast to ^{123}I-MIBG uptake, the decrease in ^{11}C-CFT uptake in the whole striatum and in each of its three subregions significantly correlated with disease progression represented by the HY stages, as reported previously [14, 16, 22]. Considering the causal pathophysiological mechanism of PD, this is reasonable because ^{11}C-CFT uptake directly indicates nigrostriatal dopaminergic function.

We investigated the sensitivity and specificity of cardiac ^{123}I-MIBG scintigraphy in diagnosing PD and differentiating the patients with PD from the other patients with chief complaints of parkinsonian symptoms. Similar to the

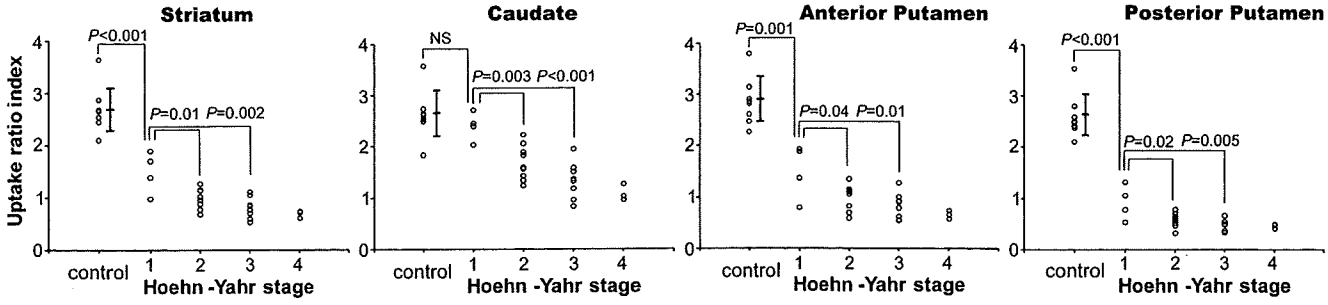

Fig. 4 Relation between the HY stage and uptake ratio index of ^{11}C-CFT in the whole striatum, caudate, anterior putamen and posterior putamen of patients with PD. In all four graphs, the uptakes in the patients in HY 1 of PD are significantly higher than those in the patients in HY 2 and 3 of PD. The uptakes in the caudate of patients in HY 1 of PD are not significantly higher than those in the caudate of controls, while the uptakes in the whole striatum, anterior putamen and posterior putamen of patients in HY 1 of PD are significantly higher than those in the corresponding regions of the controls. The *vertical bar* represents the mean ± SD of controls. *NS* not significant

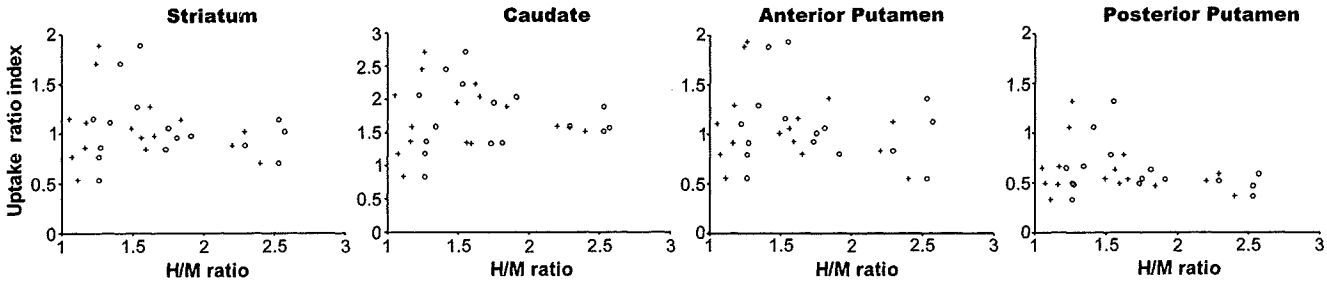

Fig. 5 Relation between the H/M ratio and uptake ratio index of ^{11}C-CFT in the whole striatum, caudate, anterior putamen and posterior putamen of patients with PD. Correlation was evaluated for 16 patients who underwent the two examinations (scintigraphy and PET) within 6 months. In all four graphs, no significant correlations are observed between the early images (*open circles*) and delayed images (*plus signs*)

previous meta-analysis of studies with a total of 246 PD cases [36], in both early and delayed images our study showed high specificity for the overall cases and high sensitivity for the advanced cases. However, early cases tended to have relatively lower sensitivity in both images, although the sample size and methodology greatly differed among the studies. Thus, our results suggested that even in the case of sustained cardiac ^{123}I-MIBG uptake, the possibility of PD should not be denied and follow-up clinical examinations, including ^{123}I-MIBG scintigraphy, should be conducted, especially in early and mild PD cases.

No definite correlation was found either between cardiac ^{123}I-MIBG uptake and striatal ^{11}C-CFT uptake or between cardiac ^{123}I-MIBG uptake and subregional ^{11}C-CFT uptake in the PD group. Two groups have reported the association between the functional impairment of the nigrostriatal dopaminergic system and that of the cardiac sympathetic system [8, 37]. Spiegel et al. (n=18) found a correlation between the two indices, i.e. ^{123}I-MIBG and ^{11}C-CFT uptake, while Raffel et al. (n=9) found no correlation between them. This discrepancy may be explained as follows. The functional impairment of both the nigrostriatal dopaminergic and cardiac sympathetic systems increases with disease progression, as described earlier; hence, a correlation was observed in some studies. On the other hand, there is no report that suggests a direct cause-effect relationship between the functional impairment of the nigrostriatal dopaminergic system and that of the cardiac sympathetic system. Thus, a statistically significant correlation between the functional impairments of the two systems may depend on the sample size and methodology. However, the functional impairments of the two systems would, in fact, occur and progress independently. Sometimes, impairment of the cardiac sympathetic function may precede that of the nigrostriatal dopaminergic function, while at other times, the latter may precede the former.

This is the first report wherein PD and NPD patterns in dopamine PET findings were defined on the basis of the results which have been confirmed as follows. In presynaptic DAT images, three characteristic changes are observed [14–16, 22]. First, the reduction in the ^{11}C-CFT uptake in the striatum begins from the posterior putamen, representing the initial locus of PD [38]. Second, the uptake ratio of the posterior putamen to the caudate is less than 1. Third, one putamen is usually more affected than the other, reflecting asymmetric degeneration. In fact, Fig. 4 shows that the ^{11}C-CFT uptake in the posterior putamen markedly decreased in the early stage of PD, while that in the caudate was relatively constant in the early stage. In postsynaptic D_2R images, putaminal uptake is normal or mildly upregulated in untreated PD, presumably as a compensatory response to decrease in presynaptic dopamine [17–19]. On the other hand, in treated or longstanding PD, the uptake restores to the normal level in the putamen and most often decreases in the caudate; this is presumably as a result of long-term downregulation due to chronic dopaminergic therapy or structural adaptation of the postsynaptic dopaminergic system to the progressive degeneration of nigrostriatal neurons [17, 19, 21]. In fact, in vitro studies have reported that the densities of striatal D_2Rs are maintained even in the advanced stage [39, 40].

On the basis of the earlier mentioned characteristic changes, especially in the posterior putamen, we defined the PD and NPD patterns such that false-negative cases should be as few as possible, because the aim was to reinforce the published clinical criteria. For defining the PD pattern, we considered that ^{11}C-CFT uptake in the posterior putamen of the patients should be less than that in the caudate of the patients and less than 50% of the mean uptake in normal controls. This percentage (i.e. 50%) was selected (1) on the basis of previous PET reports and considered suitable to distinguish normal from affected individuals [14–16, 22] and (2) on the basis of previous reports of in vitro studies, stating that parkinsonian symptoms appear when 80% of the striatal dopamine is lost or 50% of the nigral cells degenerate [38, 41]. Asymmetric uptake was not defined because of the difficulty in determining the intraindividual differences in

the uptake on the left and right sides. However, all 24 patients with PD showed asymmetric uptake. In the ^{11}C-raclopride PET image, since the uptake in the putamen was not less than the normal range, we considered that the uptake in the posterior putamen was normal or increased. For defining the NPD pattern, presynaptic function was not determined because the degree of the presynaptic dysfunction varies with diseases. In the ^{11}C-raclopride PET image, we considered that the uptake in the posterior putamen was normal or decreased because the uptake was not more than the normal range, except for Lewy body disease.

Conclusions

In early and mild PD cases, cardiac ^{123}I-MIBG scintigraphy is of limited value in the diagnosis of PD, because the sensitivity was indicated to be less than 70%. However, because of its high specificity for the overall cases and high sensitivity for the advanced cases, cardiac ^{123}I-MIBG scintigraphy may assist in the diagnosis of PD in a complementary role with the dopaminergic neuroimaging. Disease progression indicated by the HY stages has a stronger association with the nigrostriatal dopaminergic function assessed by striatal ^{11}C-CFT uptake than with the cardiac sympathetic function assessed by cardiac ^{123}I-MIBG uptake. The impairment of the two functions would occur and progress independently.

Acknowledgments The authors thank Mr. Keiichi Kawasaki, Dr. Masaya Hashimoto, and Ms. Hiroko Tsukinari for their technical assistance and useful discussions. This work was supported by grant-in-aid for Scientific Research (B) No. 20390334 (Ki.I.) from the Japan Society for the Promotion of Science and a grant (06-46) (Ki.I.) from the Program for Promotion of Fundamental Studies in Health Sciences of the National Institute of Biomedical Innovation of Japan, and a grant-in-aid for Neurological and Psychiatric Research (S.M., Y.S., and Ke.I.), and Research fo Longevity (S.M., Y.S., and Ke.I.) from the Ministry of Health, Labor, and Welfare of Japan, a grant-in-aid for Long-Term Comprehensive Research on Age-associated Dementia from the Tokyo Metropolitan Institute of Gerontology (K.K., S.M., and Ke.I.).

References

1. Orimo S, Ozawa E, Nakade S, Sugimoto T, Mizusawa H. (123)I-metaiodobenzylguanidine myocardial scintigraphy in Parkinson's disease. J Neurol Neurosurg Psychiatry 1999;67:189–94.
2. Satoh A, Serita T, Seto M, Tomita I, Satoh H, Iwanaga K, et al. Loss of 123I-MIBG uptake by the heart in Parkinson's disease: assessment of cardiac sympathetic denervation and diagnostic value. J Nucl Med 1999;40:371–5.
3. Taki J, Nakajima K, Hwang EH, Matsunari I, Komai K, Yoshita M, et al. Peripheral sympathetic dysfunction in patients with Parkinson's disease without autonomic failure is heart selective and disease specific. taki@med.kanazawa-u.ac.jp. Eur J Nucl Med 2000;27:566–73.
4. Takatsu H, Nishida H, Matsuo H, Watanabe S, Nagashima K, Wada H, et al. Cardiac sympathetic denervation from the early stage of Parkinson's disease: clinical and experimental studies with radiolabeled MIBG. J Nucl Med 2000;41:71–7.
5. Nagayama H, Hamamoto M, Ueda M, Nagashima J, Katayama Y. Reliability of MIBG myocardial scintigraphy in the diagnosis of Parkinson's disease. J Neurol Neurosurg Psychiatry 2005;76:249–51.
6. Hamada K, Hirayama M, Watanabe H, Kobayashi R, Ito H, Ieda T, et al. Onset age and severity of motor impairment are associated with reduction of myocardial 123I-MIBG uptake in Parkinson's disease. J Neurol Neurosurg Psychiatry 2003;74:423–6.
7. Braune S, Reinhardt M, Schnitzer R, Riedel A, Lucking CH. Cardiac uptake of [123I]MIBG separates Parkinson's disease from multiple system atrophy. Neurology 1999;53:1020–5.
8. Raffel DM, Koeppe RA, Little R, Wang CN, Liu S, Junck L, et al. PET measurement of cardiac and nigrostriatal denervation in Parkinsonian syndromes. J Nucl Med 2006;47:1769–77.
9. Rajput AH, Rozdilsky B, Rajput A. Accuracy of clinical diagnosis in parkinsonism–a prospective study. Can J Neurol Sci 1991;18:275–8.
10. Hughes AJ, Daniel SE, Kilford L, Lees AJ. Accuracy of clinical diagnosis of idiopathic Parkinson's disease: a clinico-pathological study of 100 cases. J Neurol Neurosurg Psychiatry 1992;55:181–4.
11. Jankovic J, Rajput AH, McDermott MP, Perl DP. The evolution of diagnosis in early Parkinson disease. Parkinson Study Group. Arch Neurol 2000;57:369–72.
12. Hughes AJ, Daniel SE, Lees AJ. Improved accuracy of clinical diagnosis of Lewy body Parkinson's disease. Neurology 2001;57:1497–9.
13. Plotkin M, Amthauer H, Klaffke S, Kuhn A, Ludemann L, Arnold G, et al. Combined 123I-FP-CIT and 123I-IBZM SPECT for the diagnosis of parkinsonian syndromes: study on 72 patients. J Neural Transm 2005;112:677–92.
14. Nurmi E, Bergman J, Eskola O, Solin O, Vahlberg T, Sonninen P, et al. Progression of dopaminergic hypofunction in striatal subregions in Parkinson's disease using [18F]CFT PET. Synapse 2003;48:109–15.
15. Frost JJ, Rosier AJ, Reich SG, Smith JS, Ehlers MD, Snyder SH, et al. Positron emission tomographic imaging of the dopamine transporter with 11C-WIN 35,428 reveals marked declines in mild Parkinson's disease. Ann Neurol 1993;34:423–31.
16. Rinne JO, Ruottinen H, Bergman J, Haaparanta M, Sonninen P, Solin O. Usefulness of a dopamine transporter PET ligand [(18)F] beta-CFT in assessing disability in Parkinson's disease. J Neurol Neurosurg Psychiatry 1999;67:737–41.
17. Antonini A, Schwarz J, Oertel WH, Beer HF, Madeja UD, Leenders KL. [11C]raclopride and positron emission tomography in previously untreated patients with Parkinson's disease: influence of L-dopa and lisuride therapy on striatal dopamine D2-receptors. Neurology 1994;44:1325–9.
18. Kaasinen V, Ruottinen HM, Någren K, Lehikoinen P, Oikonen V, Rinne JO. Upregulation of putaminal dopamine D2 receptors in early Parkinson's disease: a comparative PET study with [11C] raclopride and [11C]N-methylspiperone. J Nucl Med 2000;41:65–70.
19. Rinne JO, Laihinen A, Rinne UK, Någren K, Bergman J, Ruotsalainen U. PET study on striatal dopamine D2 receptor changes during the progression of early Parkinson's disease. Mov Disord 1993;8:134–8.
20. Dentresangle C, Veyre L, Le Bars D, Pierre C, Lavenne F, Pollak P, et al. Striatal D2 dopamine receptor status in Parkinson's disease: an [18F]dopa and [11C]raclopride PET study. Mov Disord 1999;14:1025–30.
21. Antonini A, Schwarz J, Oertel WH, Pogarell O, Leenders KL. Long-term changes of striatal dopamine D2 receptors in patients

with Parkinson's disease: a study with positron emission tomography and [11C]raclopride. Mov Disord 1997;12:33–8.
22. Wang J, Zuo CT, Jiang YP, Guan YH, Chen ZP, Xiang JD, et al. 18F-FP-CIT PET imaging and SPM analysis of dopamine transporters in Parkinson's disease in various Hoehn & Yahr stages. J Neurol 2007;254:185–90.
23. Knudsen GM, Karlsborg M, Thomsen G, Krabbe K, Regeur L, Nygaard T, et al. Imaging of dopamine transporters and D2 receptors in patients with Parkinson's disease and multiple system atrophy. Eur J Nucl Med Mol Imaging 2004;31:1631–8.
24. Kim YJ, Ichise M, Ballinger JR, Vines D, Erami SS, Tatschida T, et al. Combination of dopamine transporter and D2 receptor SPECT in the diagnostic evaluation of PD, MSA, and PSP. Mov Disord 2002;17:303–12.
25. Verstappen CC, Bloem BR, Haaxma CA, Oyen WJ, Horstink MW. Diagnostic value of asymmetric striatal D2 receptor upregulation in Parkinson's disease: an [123I]IBZM and [123I]FP-CIT SPECT study. Eur J Nucl Med Mol Imaging 2007;34:502–7.
26. Fujiwara T, Watanuki S, Yamamoto S, Miyake M, Seo S, Itoh M, et al. Performance evaluation of a large axial field-of-view PET scanner: SET-2400W. Ann Nucl Med 1997;11:307–13.
27. Hashimoto M, Kawasaki K, Suzuki M, Mitani K, Murayama S, Mishina M, et al. Presynaptic and postsynaptic nigrostriatal dopaminergic functions in multiple system atrophy. Neuroreport 2008;19:145–50.
28. Ishibashi K, Ishii K, Oda K, Kawasaki K, Mizusawa H, Ishiwata K. Regional analysis of age-related decline in dopamine transporters and dopamine D2-like receptors in human striatum. Synapse 2009;63:282–90.
29. NK LO, Dolle F, Lundkvist C, Sandell J, Swahn CG, Vaufrey F, et al. Precursor synthesis and radiolabelling of the dopamine D2 receptor ligand [11C]raclopride from [11C]methyl triflate. J Labelled Compd Radiopharm 1999;42:1183–93.
30. Kawamura K, Oda K, Ishiwata K. Age-related changes of the [11C]CFT binding to the striatal dopamine transporters in the Fischer 344 rats: a PET study. Ann Nucl Med 2003;17:249–53.
31. Antonini A, Leenders KL, Reist H, Thomann R, Beer HF, Locher J. Effect of age on D2 dopamine receptors in normal human brain measured by positron emission tomography and 11C-raclopride. Arch Neurol 1993;50:474–80.
32. Nakajima K, Taki J, Tonami N, Hisada K. Decreased 123I-MIBG uptake and increased clearance in various cardiac diseases. Nucl Med Commun 1994;15:317–23.
33. Gilman S, Low PA, Quinn N, Albanese A, Ben-Shlomo Y, Fowler CJ, et al. Consensus statement on the diagnosis of multiple system atrophy. J Auton Nerv Syst 1998;74:189–92.
34. Litvan I, Agid Y, Calne D, Campbell G, Dubois B, Duvoisin RC, et al. Clinical research criteria for the diagnosis of progressive supranuclear palsy (Steele-Richardson-Olszewski syndrome): report of the NINDS-SPSP international workshop. Neurology 1996;47:1–9.
35. Li ST, Dendi R, Holmes C, Goldstein DS. Progressive loss of cardiac sympathetic innervation in Parkinson's disease. Ann Neurol 2002;52:220–3.
36. Braune S. The role of cardiac metaiodobenzylguanidine uptake in the differential diagnosis of parkinsonian syndromes. Clin Auton Res 2001;11:351–5.
37. Spiegel J, Mollers MO, Jost WH, Fuss G, Samnick S, Dillmann U, et al. FP-CIT and MIBG scintigraphy in early Parkinson's disease. Mov Disord 2005;20:552–61.
38. Fearnley JM, Lees AJ. Ageing and Parkinson's disease: substantia nigra regional selectivity. Brain 1991;114(Pt 5):2283–301.
39. Guttman M, Seeman P, Reynolds GP, Riederer P, Jellinger K, Tourtellotte WW. Dopamine D2 receptor density remains constant in treated Parkinson's disease. Ann Neurol 1986;19:487–92.
40. Bokobza B, Ruberg M, Scatton B, Javoy-Agid F, Agid Y. [3H] spiperone binding, dopamine and HVA concentrations in Parkinson's disease and supranuclear palsy. Eur J Pharmacol 1984;99:167–75.
41. Kish SJ, Shannak K, Hornykiewicz O. Uneven pattern of dopamine loss in the striatum of patients with idiopathic Parkinson's disease. Pathophysiologic and clinical implications. N Engl J Med 1988;318:876–80.

Special Topic 4

双極性障害における神経生物学的研究

理化学研究所 脳科学総合研究センター 精神疾患動態研究チーム
加藤 忠史

Key words　うつ病／リチウム／バルプロ酸／ミトコンドリア機能障害仮説／小胞体ストレス反応

双極性障害とうつ病

双極性障害は、これまで躁うつ病と呼ばれ、統合失調症と並ぶ2大精神疾患の1つとされてきた。躁状態、うつ状態の再発を繰り返すことにより、深刻な社会生活障害をきたす疾患である[1]。

双極性障害は、躁病エピソードを呈する双極I型障害と、軽躁病エピソードと大うつ病エピソードを反復する双極II型障害にわけられる。躁病エピソードは、気分高揚、誇大性、活動性亢進、睡眠欲求の減少などを特徴とする。一方、同様の症状を呈するが社会的な問題とならない程度の場合を、軽躁病エピソードという。大うつ病エピソードは、抑うつ気分、興味・喜びの喪失などを主症状とし、意欲低下、希死念慮、罪責感などの精神症状、不眠、食欲低下、易疲労感などの身体症状を特徴とする。

双極性障害の発症年齢の平均はおよそ30歳であるが、幅広い年齢で発症することが確認されており、明らかな男女差はない。生涯罹患率は0.4～2%程度とされている。病相の間隔は、発症時には平均5年程度であるが、再発の度に再発までの間隔が短縮するという特徴がある。

一卵性双生児の一致率が二卵性双生児に比して高いことなどから、遺伝要因の関与が明らかにされており、その特徴的な症状と合わせ、精神疾患のなかでもとくに生物学的な要素の強い疾患と考えられている。

双極性障害の治療には気分安定薬が用いられ、なかでもリチウムはもっとも確立した治療薬である。その他、バルプロ酸、カルバマゼピンなどが、気分安定薬として広く用いられる。また、クエチアピン、オランザピンなどの非定型抗精神病薬の有効性も報告されている。

しかしながら、第一選択薬であるリチウムは副作用が強いため、服薬中断に至ることも少なくない。また、これらの気分安定薬を併用しても、病相が完全にコントロールできない患者も少なくなく、とくにうつ病相には有効な薬剤が少ないのが現状である。

うつ病は、社会生活の障害をきたす最大の要因となっている疾患である。しかし、その治療法は未だ確立されておらず、既存の薬剤に反応しない難治性の患者が多い。さらに、抗うつ薬服用後に、焦燥感や衝動性が悪化する事例が少なくないことが社会問題になっている[2]。これは、うつ病患者のなかに含まれる潜在的な双極性障害患者、すなわち双極スペクトラムである者が、抗うつ薬で躁転などの悪化をきたすためであることが指摘され、現在ではすべての抗うつ薬に、躁うつ病患者に対しては慎重に投与すべきであると明記されている。現実の臨床においては、こうした症例では、最初から抗うつ

Author 著者

加藤 忠史
理化学研究所 脳科学総合研究センター
精神疾患動態研究チーム チームリーダー

東京大学医学部卒。同附属病院、滋賀医科大学精神医学教室、東京大学医学部附属病院精神神経科を経て、2001年より現職。著書に「双極性障害」「うつ病の脳科学」「脳と精神疾患」「こころだってからだです」。

研究チームのホームページ
http://www.brain.riken.go.jp/jp/t_kato.html
個人ホームページ
http://square.umin.ac.jp/tadafumi

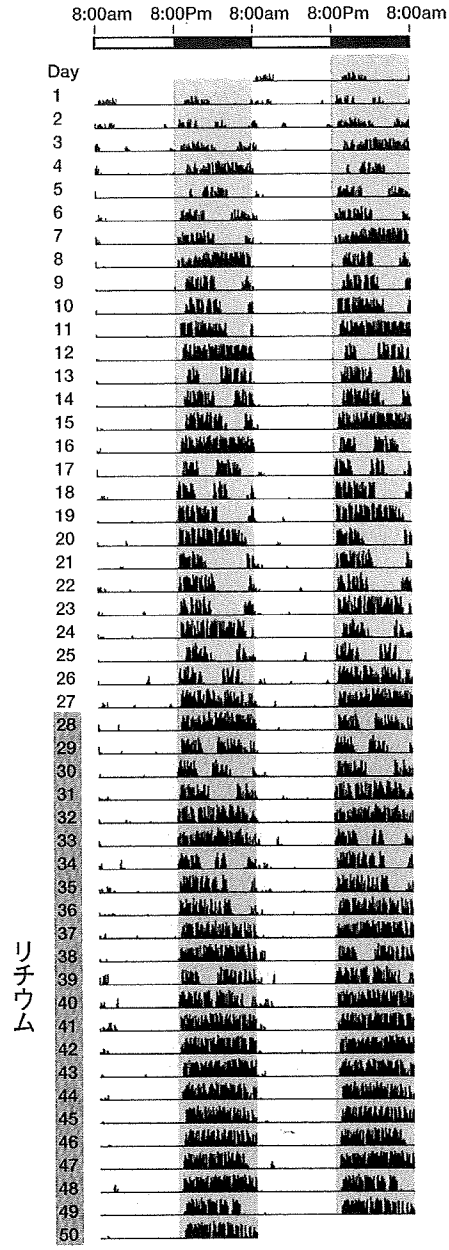

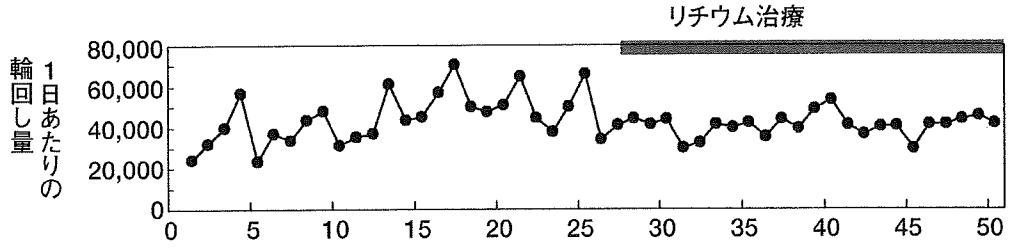

図1　変異Polgトランスジェニックマウスにおける行動リズムの変化

性周期に伴う、周期的な輪回し行動量の変化がみられた。この周期的行動量変化は、リチウム投与により改善した。

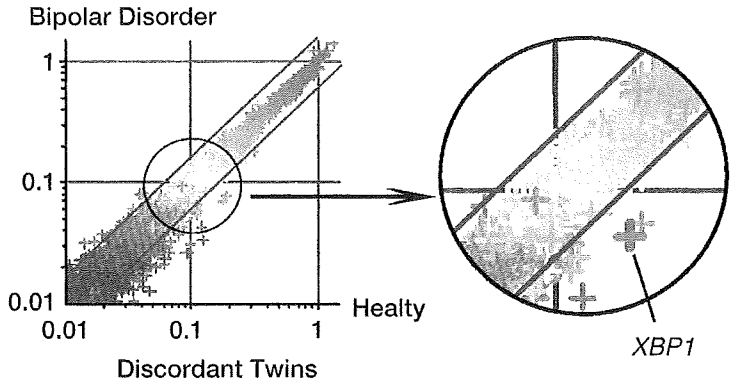

図2　双極性障害に関して不一致な、
一卵性双生児の培養リンパ芽球における遺伝子発現解析

薬でなく気分安定薬を用いる場合も多い。

リチウムが単純なイオンであるために、構造を変化させて類似薬を作ることができなかったことに加え、確立した双極性障害の動物モデルがなかったことから、新たな気分安定薬の開発は、他疾患の治療薬の適応拡大を除けば、世界的にほとんど行われていない。

このように、双極性障害を早期に診断する方法の開発や、副作用の少ない気分安定薬の開発などが急務である。そして、診断法や治療法の開発のためには、何よりも双極性障害の病因を解明することが必要である。

気分安定薬の薬理学

これまでの研究により、気分安定薬であるリチウムとバルプロ酸が共通に神経保護作用を持つことが指摘されている。そのメカニズムとしては、細胞内イノシトール枯渇作用、Bcl-2(B-cell lymphoma 2)増加、GSK3β(glycogen synthase kinase 3β)阻害、BDNF(brain-derived neurotrophic factor)増加など、多数のメカニズムが報告されており、これらのうちどれが重要であるかについては、一致した見解には至っていない[3]。

最近、双極性障害に対して抗躁効果、病相予防効果、および抗うつ効果を有することが明らかにされた非定型抗精神病薬も、気分安定薬と同様の神経保護作用を持つことが明らかにされている。

ミトコンドリア機能障害仮説

我々は、双極性障害患者における磁気共鳴スペクトロスコピー所見がミトコンドリア病CPEO(慢性進行性外眼筋麻痺)に類似していることや、患者死後脳でミトコンドリアDNA(mtDNA)欠失が検出されたことなどから、脳内のmtDNA変異蓄積が双極性障害の病態に関与するとの「ミトコンドリア機能障害仮説」を提唱した[4]。

CPEOは、眼瞼下垂、眼球運動障害などを呈するまれな遺伝病であり、骨格筋にmtDNA欠失が蓄積することがその原因と考えられてきたが、症状の1つとして気分障害を呈する場合がある。こうした患者では、脳にもmtDNA欠失が蓄積していたと報告されている。CPEOは、mtDNAの維持に関連するいくつかの核遺伝子の変異によって発症する遺伝病であるが、その原因遺伝子の1つは、mtDNA合成酵素(POLG)である。

我々は、神経細胞特異的にPOLG変異を発現するトランスジェニックマウスを作製した。このマウスでは、脳内にmtDNA欠失が蓄積していた。このマウスは、概日リズム障害、周期的行動量変化などの双極性障害に類似する表現型を示した。また、リチウム投与により、これらの行動変化が改善した(図1)。また、三環系抗うつ薬の投与により、躁転に類似した行動変化を示した[5]。

双極性うつ病に対して、リチウム以外に確実な効果を示す治療法には電気けいれん療法(ECT)があるが、この方法によって、モデルマウスは顕著に行動異常が改善した。

これらのことから、このマウスは、構成的妥当性(原因の共通性)、表面妥当性(行動変化の類似性)、および予測妥当性(治療薬の有効性)を満たす、双極性障害のモデルマウスとな

りうると考えられた。

双極性障害のミトコンドリア機能障害仮説は、患者の死後の脳において、ミトコンドリア関連核遺伝子の発現低下がみられるという報告[6]を契機に、海外の研究者にも支持されるようになった。

小胞体ストレス反応

一方で我々は、一卵性双生児不一致例における遺伝子発現解析から、双極性障害におけるXBP1(x-box binding protein 1)の役割に注目し、双極性障害患者由来培養リンパ芽球では小胞体ストレスに対するXBP1誘導が低下していることを示した[7](図2)。

XBP1ノックアウトマウス由来の初代培養神経細胞では、BDNF(脳由来神経栄養因子)による神経突起伸展、およびGABAニューロンマーカーの発現増加反応が減弱していることから、XBP1は神経細胞、特にGABAニューロンの発達に関与する可能性が考えられた[8]。

気分安定神経系仮説

これらの研究から、双極性障害においては、ミトコンドリア機能障害および小胞体ストレス反応の障害による神経細胞の脆弱性が、その病態に関与している可能性が考えられた。

しかしながら、POLG変異はミトコンドリア病のみならず、パーキンソン病などの多くの疾患との関連も推定されており、決して双極性障害に特異的なものではない。POLG変異によって脳内の気分調節にかかわる神経系が次第に障害され、双極性障害を発症すると考えれば納得がいく。この「気分安定神経系」仮説は、病相を繰り返すにしたがって再発間隔が短縮し、急速交代化するともはや気分安定薬は奏功しないという、双極性障害の特徴的な臨床経過をよく説明している。

双極性障害の原因を特定し、特異的診断法・治療法を開発するためには、POLG変異により障害される神経系を特定し、双極性障害の最終共通経路となる脳病態を解明する必要がある。

mtDNA欠失を持つ細胞では、次第に欠失mtDNAが野生型mtDNAよりも優勢となっていく現象が報告されている。これは、欠失mtDNAの方が野生型よりも短く、複製速度が速いためと考えられる。分化後の、核DNAの合成を行っていない神経細胞でも、mtDNAは合成され続けていると考えられる。

ストレスで海馬神経細胞の樹状突起が萎縮することが報告されているが、特に環境に適応するために可塑的変化を繰り返すような神経系でmtDNA欠失が蓄積しやすく、こうした神経系が次第に機能停止に至ることが双極性障害の原因になるのかも知れない[9]。

おわりに—今後の方向性

POLG変異によってmtDNA欠失が蓄積し、それに伴って双極性障害様の行動変化を示すような神経系を探索することにより、双極性障害の原因脳部位を同定することが可能かもしれない。これらの脳部位において形態学的変化をきたしている細胞の特徴を特定し、最終的にこの神経病理学的所見をヒト死後脳において確認することができれば、双極性障害の原因神経系同定につながると期待される。

双極性障害のような主要な精神疾患を神経病理学的に定義することは、双極性障害研究の大きな進歩となるだけでなく、精神医学の新たなるスタートになることが期待される。

[参考文献]

1) 加藤忠史:双極性障害:ちくま新書, 2009.
2) 加藤忠史:うつ病の脳科学:幻冬舎新書, 2009.
3) 加藤忠史:脳と精神疾患:朝倉書店, 2009.
4) Kato T, et al.: Mitochondrial dysfunction in bipolar disorder. Bipolar Disorder 2: 180-190,2000.
5) Kasahara T, et al.: Mice with neuron-specific accumulation of mitochondrial DNA mutations show mood disorder-like phenotypes. Mol Psychiatry 11: 577-593,2006.
6) Konradi C, et al.: Molecular evidence for mitochondrial dysfunction in bipolar disorder. Arch Gen Psychiatry 61: 300-308,2004.
7) Hayashi A, et al.: Aberrant endoplasmic reticulum stress response in lymphoblastoid cells from patients with bipolar disorder. Int J Neuropsychopharmacol 12: 33-43,2009.
8) Hayashi A, et al : Attenuated BDNF-induced upregulation of GABAergic markers in neurons lacking Xbp1. Biochem Biophys Res Commun 376: 758-763,2008.
9) Kato T, et al.: Molecular neurobiology of bipolar disorder,Trends Neurosci 31: 495-503,2008.

うつ病の分子生物学的研究

Molecular biology of depression

加藤忠史
Tadafumi Kato
理化学研究所脳科学総合研究センター精神疾患動態研究チーム

◎うつ病は遺伝子，性格，養育，ストレス，身体因，薬剤など，多様な要因が複雑にからみあって発症する症候群であり，その分子生物学的研究には多様な方法と視点が必要となる．セロトニントランスポーター遺伝子とストレス・養育要因との相互作用，セロトニン合成酵素のまれな変異との関連など，興味深い報告がなされたが，その後の追試では確認されていない．ストレス脆弱性にDNAメチル化の関与が疑われている．抗うつ薬の作用メカニズムの研究から，うつ病では神経細胞が形態レベルで変化しており，抗うつ薬がこれを是正するという仮説が提示され，現在この方向での研究が多く行われている．

Key word：うつ病，セロトニン，BDNF，DNAメチル化

うつ病の分子生物学的研究のストラテジー

うつ病の発症要因は，遺伝的基盤，病前性格，養育がストレス脆弱性に与える影響，ストレスが脳に与える影響，うつ病の危険因子となる身体因および薬剤など，多様である(図1)．

一方，うつ病の治療としては，抗うつ薬，電気けいれん療法，TMS(経頭蓋磁気刺激)，認知行動療法などがあり，こうした治療法の作用機転も研究対象となる．

患者の病態を直接調べる方法としては，遺伝学，脳画像法，生理学的測定，神経内分泌学的試験，脳脊髄液の測定，血液の測定，血液細胞の測定，死後脳研究など，さまざまな方法がある．これらの研究方法により得られた所見には，素因依存性の所見，すなわちうつ状態の有無にかかわらずみられ，うつ病へのかかりやすさ(脆弱性)を反映する所見と，状態依存性の所見(うつ状態を直接反映する所見)とがある．これらに加え，脆弱性をもつだけではみられないが，発症後は状態にかかわりなくみられるようになる所見，すなわち発症マーカーともいうべき所見も存在する可能性がある．

また，うつ病は単一の疾患ではなく，異種性の高い症候群というべきものであり，これらに共通な部分が想定されると同時に，各亜型に特異的な病態も存在する．たとえば，いわゆる内因性うつ病(メランコリー型)，非定型うつ病，季節性うつ病，いわゆる血管性うつ病，双極スペクトラムうつ病など，それぞれ異なった生物学的背景をもっている．

このように，うつ病とはさまざまな遺伝・環境要因が発症に関与し，多様な治療法が存在する症候群であり，さまざまな研究手法により得られる所見には状態依存性と素因依存性の所見が混在しているとともに，うつ状態に共通な所見とうつ病の亜型に特異的な所見とが共存していると考えられる．

したがって，うつ病の分子生物学的研究のストラテジーは多岐にわたり，そのデータの解釈にも注意が必要だと考えられる．本特集では遺伝子，神経内分泌，ストレス，ゲノム創薬，画像，NIRS，器質因，睡眠と，うつ病にかかわるほとんどの研究手法が網羅されているため，詳細は各項に譲るとして，本稿ではこれらの間の相互関係を分子生物学的視点から解き明かすことを主眼としたい．

263-01475

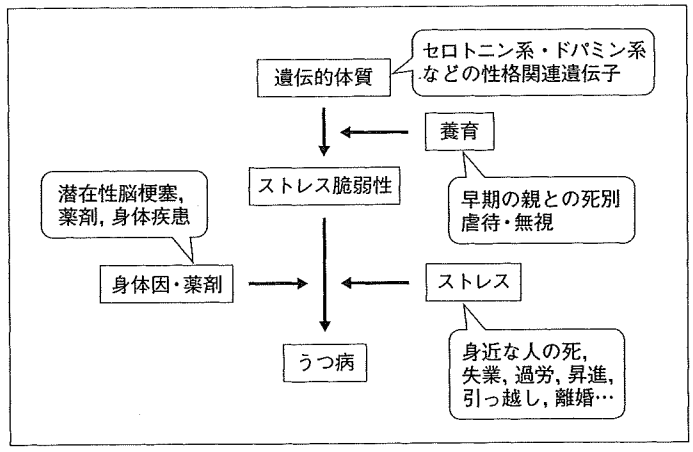

図 1　うつ病の発症メカニズム

遺伝-環境相互作用

うつ病の危険因子(リスクファクター)として，歴史的には執着性格やメランコリー型などの性格要因と状況因，すなわちある性格をもつ人に固有のストレス因子というべきものが重要視されてきた．一方，双生児研究，家族研究から，うつ病の発症に遺伝的要因がかかわることも明らかであり，遺伝要因により説明できる部分は統合失調症や双極性障害に比べると低いものの，3〜4 割であると考えられている[1]．性格と遺伝子の関係に関する多くの研究から，遺伝的危険因子が性格を介して発症するとのモデルでとらえられるようになり[2]，性格と状況因という古典的なうつ病の考え方は，遺伝-環境相互作用という文脈で研究されるようになってきた．

Caspi ら[3]は，セロトニントランスポーターのプロモーター多型(HTTLPR)の個人差により，ストレスを受けたときにうつ病を発症する率が異なることを 847 名という多数例の前向き研究により示した．同様の関係は虐待についてもみられ，S 型をもつことが虐待を受けたときにうつ病を発症することと関係していた．彼らがセロトニントランスポーターに着目したのは，これが抗うつ薬の標的分子と考えられているためである．シナプス前より放出されたセロトニンは，セロトニントランスポーターを介して再度取り込まれて分解される．このセロトニントランスポーター遺伝子の上流のプロモーターに，遺伝子発現量を変化させる S 型と L 型の 2 種類がある(HTTLPR)とされ，精神医学領域でもっともよく研究された遺伝子多型となっている．とくに，発現量の少ない S 型が神経症傾向などの性格と関連していると報告されていることから，うつ病との関連も考えられたが，遺伝子関連研究では一致した結果が得られていなかった．Caspi らは，環境要因を考慮に入れることで，より明確な結論を得たと考えられたのである．

この研究は，うつ病における遺伝-環境相互作用をはじめて明確に示した研究として大きな関心を引いたが，その後の研究ではサンプル数の小さな論文では支持する結果も報告されたものの，より大きなサンプル数(4,175 名)での研究ではこうした遺伝-環境相互作用は否定された[4]．

さらに，この S/L 多型は，PET により測定される脳内セロトニントランスポーター結合に影響しないこと[5]，HTTLPR の多型は S 型と L 型の 2 つではなく，14 種類のアリルからなり，それぞれ機能の異なる複雑な多型であること[6]から S 型，L 型の 2 分法での研究自体に疑問が生じているのが現状である．

一方，心血管系の危険因子(動脈硬化，高脂血症)などの身体的要因やインターフェロンなどの薬剤もうつ病の危険因子となり，食生活などの環境と相互作用してうつ病発症に関与すると考えられることから，これら内科領域の分子生物学研究も，うつ病の理解に寄与すると期待される．

263-01475

まれな遺伝子変異によるうつ病の可能性

これまでの精神疾患の遺伝子研究は common variant common disease(CVCD)仮説に基づく研究が多く，こうした場合に遺伝-環境相互作用が問題となる．一方，まれな遺伝子変異があると，環境因の有無にかかわりなく精神疾患を発症するという場合も考えられ，こうした multiple rare variant common disease(MRVCD)仮説に基づく研究も行われている．

セロトニン合成酵素であるトリプトファンヒドロキシラーゼの遺伝子，TPH のホモログとして見出された TPH2 が脳に選択的に発現していることがわかり，その病因的意義に関心が集まり，研究が行われた．その結果，TPH2 遺伝子の機能喪失変異(G1463A，R441H)が 87 名のうつ病患者中 9 名に存在し，219 名の健常対照群では 1 人もみられないと報告され[7]，大きな関心をよび起こした．しかし，その後の多くの研究で，この所見は再現されなかった．

ストレスとストレス脆弱性

ストレスは視床下部-下垂体-副腎皮質系(HPA 系)に影響するが，うつ病患者ではデキサメタゾン抑制試験の異常などから HPA 系のネガティブフィードバックが障害されていると考えられており，グルココルチコイド受容体が抗うつ治療のターゲットとしても検討されている．

虐待経験のあるうつ病患者では HPA 系のフィードバック障害がみられることなどから[8]，幼少期の養育がこの系に影響を与え，うつ病への脆弱性が形成されると考えられている．Meaney らのグループは，あまり子育てをしないラットの仔はストレス耐性が低くなり，これが海馬グルココルチコイド受容体の発現量低下による視床下部-下垂体-副腎皮質系のフィードバック機能変化を介していると考えて研究を進めている．さらに彼らは，養育行動の程度により仔のグルココルチコイド受容体遺伝子のプロモーター領域の DNA メチル化が変化することがその分子メカニズムであると報告し，注目された[9]．

ゲノム DNA は CpG アイランドの CpG 部分の C(シトシン)がメチル化修飾を受けるかどうかによって，近傍の遺伝子の発現量が変化する．DNA メチル化状態は発達後はある程度安定していると考えられるが，受精卵でいったん消去されリプログラミングされることから，発生初期には不安定な状態にあると想像される．そのため，DNA メチル化が発生初期の環境との相互作用を記憶する役割を果たしていると想像されるのである．しかし，前述の論文後，他のグループによる追試の報告はない．その後，同グループからヒト死後脳研究の結果が発表され，虐待を受けた者では，グルココルチコイド受容体遺伝子の DNA メチル化が高かったと報告された[10]．しかし，ラットで変化の見られた部位(NGFI-A 結合部位)には全くメチル化は見られず，その上流の 2 サイトに差があり，「この部位は NGFI-A 結合部位ではないが，そのメチル化は NGFI-A による転写活性に影響する」というデータであったことから，さらなる検討が必要と思われる．いずれにせよ，ストレス脆弱性の分子基盤に DNA メチル化が関与しているかどうかはまだまだデータ不足といわざるをえないのが現状である．

抗うつ薬の作用メカニズム

抗精神病薬として開発されたイミプラミンが抗うつ作用をもつことが臨床試験のなかから見出され，これがセロトニン，ノルアドレナリンの取込み阻害作用をもっていたこと，結核の治療に用いられていた INH が気分高揚作用をもち，これがモノアミン酸化酵素阻害作用をもっていたことなどから，セロトニン欠乏がうつ病を引き起こし，抗うつ薬がシナプス間隙のセロトニンを増加させる作用を介して作用するというセロトニン仮説が生まれた．この理論に基づいてセロトニン選択的取込み阻害薬(SSRI)が開発され，その臨床効果が証明されたことも，この仮説を裏づけるものと考えられた．

また，抗うつ薬がシナプスでセロトニンを増やす作用は数時間以内に発現すると考えられるのに対し，臨床効果の発現には 1〜2 週間を要することから，セロトニンだけですべてを説明できるほど単純ではないと考えられるようになった．抗うつ薬投与開始後数週間で脳内に現れる変化を調べた

263-01475